SANDIA REPORT

SAND86—1813 • UC—05
Unlimited Release
Printed April 1988

Port

The Effect of Operating Temperature on Open, Multimegawatt Space Power Systems

M. W. Edenburn

Prepared by
Sandia National Laboratories
Albuquerque, New Mexico 87185 and Livermore, California 94550
for the United States Department of Energy
under Contract DE-AC04-76DP00789

BMDO

U5100

Issued by Sandia National Laboratories, operated for the United States Department of Energy by Sandia Corporation.

Printed in the United States of America
Available from
National Technical Information Service
U.S. Department of Commerce
5285 Port Royal Road
Springfield, VA 22161

NTIS price codes
Printed copy: A03
Microfiche copy: A01

Report Number: SAND86-1813
Accession Number: 5100
Title: Effect Of Operating Temperature On
Open, Multimegawatt Space Power
Systems
Personal Author: Edenburn, M.W.
Contract Number: DE-AC04-76DP00789
Report Number Assigned by Contract Monitor: UC-05
Corporate Author or Publisher: Sandia National Laboratories,
Advanced Power Systems Division,
Albuque
Report Prepared For: U.S. Department Of Energy
Publication Date: Apr 01, 1988
Pages: 28
Comments on Document: Came from Poet
Descriptors, Keywords: Effect Operate Temperature Open
Multimegawatt Space Power System
Hydrogen Oxygen Turbine Reactor
Shield Conversion Component
Combustion Burst Anti-Ballistic
Missile Weapon Inlet Mass Fuel Fluid

SAND86-1813
Unlimited Release
Printed April 1988

Distribution
Category UC-05

THE EFFECT OF OPERATING TEMPERATURE ON OPEN, MULTIMEGAWATT SPACE POWER SYSTEMS

M. W. Edenburn
Sandia National Laboratories
Advanced Power Systems Division
Albuquerque, NM 87185

ABSTRACT

In this study, we have addressed reactor-powered and combustion-powered multimegawatt, burst-mode, space power systems to evaluate the effect turbine inlet temperature will have on their performance and mass. Both systems will provide power to space-based antiballistic missile weapons that require hydrogen for cooling, and both use this hydrogen coolant as a working fluid or as a fuel for power generation. The quantity of hydrogen needed for weapon cooling increases as the weapon's cooling load increases and as weapon coolant outlet temperature decreases. Also, the hydrogen needed by the turbines in both power systems increases as turbine inlet temperature decreases. When weapon cooling loads are above 40% to 50% of weapon power and weapon coolant outlet temperature is below 300 K to 400 K, the weapon needs more hydrogen than the turbine in either the reactor- or combustion-powered systems using turbine inlet temperatures at or below the limits of current materials. There is therefore very little system mass reduction to be gained by operating a burst-mode power system at a turbine inlet temperature above present material temperature limits unless the weapon's cooling load is below 40% to 50% or coolant outlet temperature is above 300 K to 400 K. Furthermore, the combustion system's mass increases as turbine inlet temperature increases because oxygen inventory increases.

Acknowledgments

This work was performed at Sandia National Laboratories, which is operated for the U. S. Dept. of Energy under contract #DE-AC04-76DP00789, for the Strategic Defense Initiative Space Power Office's Independent Evaluation Group. Sandia is teamed with NASA's Lewis Research Center for this effort. The author is particularly thankful for Steve Hudson's assistance with power conversion modeling and for Lou Cropp's technical overview.

TABLE OF CONTENTS

LIST OF FIGURES

INTRODUCTION

We are currently evaluating multi-megawatt space power systems to help determine which areas of technical development should receive emphasis. This paper presents results from a part of our system evaluation work that deals with open, burst mode power systems. Two types of systems are considered here: (1) a hydrogen-cooled reactor-powered system and (2) a hydrogen-oxygen combustion-powered system. Both systems are open because they exhaust effluents from their power generation process into space, and both provide electrical power to space-based weapons, such as electromagnetic launchers (EML), neutral particle beams (NPB), and free electron lasers (FEL), each of which will require a few hundred megawatts for several minutes. It is generally believed that increasing a space power system's turbine inlet temperature will improve system performance and reduce mass. This paper studies the effect turbine inlet temperature has on the performance and mass of these two open, burst mode power systems.

The reactor-powered system (Figure 1) consists of a hydrogen coolant subsystem, a hydrogen-cooled reactor, a turbine, a flywheel, a generator, a power conditioning unit, and a weapon. The hydrogen coolant subsystem comprises liquid hydrogen stored at 20 K and 0.1 MPa pressure, a multifoil insulated pressure vessel, a refrigeration unit, and a meteoroid shield. The hydrogen-cooled reactor uses a moderated uranium-carbide fuel core. The flywheel stores 10 s worth of full power energy for use during transition periods. The power conditioning (PC) unit changes the generated electrical power into a form that can be used by the weapon. The PC unit's characteristics are strongly dependent on the type of weapon to be powered. An EML weapon will require almost no power conditioning because its generator will feed power directly into the weapon's circuitry. On the other hand, both NPBs and FELs will require substantial power conditioning to change the generator output into carefully regulated DC power at roughly 100 kV.

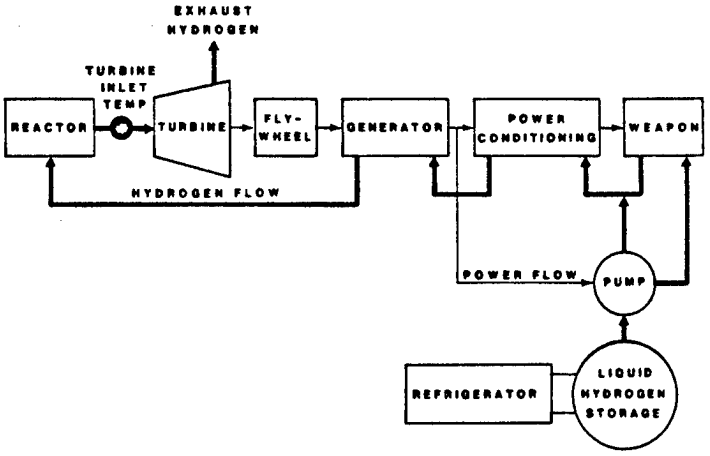

Figure 1. Burst-Mode, Reactor- Powered, Space Power System Schematic

When the weapon is operating, a pump pressurizes and supplies hydrogen coolant to the weapon. The pump's outlet pressure is equal to the turbine's inlet pressure plus any pressure losses experienced before the hydrogen enters the turbine. (The effect of high pressure on the weapon has not been considered in this analysis, but it may be important and should be considered in future analyses.) Pressurizing the hydrogen when it is a liquid requires much less power than compressing it in the gaseous state after it has cooled the weapon, and the mass of pumps is less than that of compression equipment.

The hydrogen absorbs heat in the weapon from various loss mechanisms that contribute to the weapon's inefficiency. The flow rate of hydrogen needed to cool the weapon depends on the hydrogen's outlet temperature and on the weapon's cooling load. An individual component may be primarily responsible for determining this coolant flow rate. For example, in a neutral particle beam device, the heat that must be dumped from the accelerator cavity represents only a small portion of the heat that must be dumped from the entire weapon; however, since the cavity must be kept very cold, the permissible temperature rise in the hydrogen coolant is small and its flow rate is quite large. The weapon's cooling load is the fraction of its input power that must be removed as heat. After cooling the weapon, the hydrogen cools the power conditioning unit and the generator. It then enters the reactor where it is heated to a prescribed turbine inlet temperature. After powering the turbine, the hydrogen is exhausted into space.

If the turbine needs more hydrogen than the weapon, extra hydrogen is supplied from the storage tank. If the turbine needs less hydrogen than the weapon, the turbine's pressure ratio is reduced and all of the hydrogen coming from the weapon is used.

The combustion system, Figure 2, is similar to the reactor system; but, instead of a reactor, it uses a combustion chamber and an oxygen

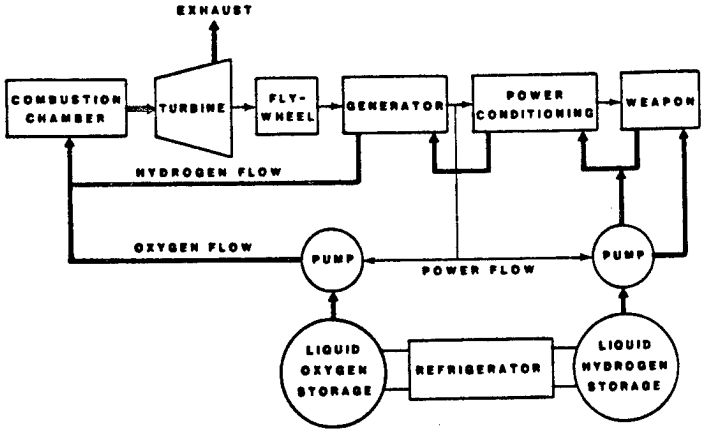

Figure 2. Burst Mode, Combustion Powered, Space Power System Schematic

supply. The combustion product temperature for a stoichiometric mixture of hydrogen and oxygen is quite high, so excess hydrogen is used to lower the temperature. A hydrogen-to-oxygen ratio is selected to give the desired combustion product temperature. As the ratio of hydrogen to oxygen decreases, the combustion product temperature increases, and the ratio of steam to hydrogen in the combustion products increases. After the combustion products power the turbine, they are exhausted into space.

We have not considered using oxygen as a coolant; however, if it can be used, the quantity of hydrogen needed in the combustion system will be reduced.

SYSTEM PERFORMANCE AND MASS CALCULATIONS

We calculated performance and mass for both types of power systems using models developed at Sandia National Laboratories and described by Edenburn (1988). The models calculate two hydrogen flow rates: (1) the flow rate necessary to cool the weapon and (2) the flow rate needed by the turbine to generate the required weapon power. Since the same hydrogen is used by the weapon first and then by the power generation system, the total hydrogen flow rate needed is the greater of the two above flow rates. The flow rates are calculated using temperature dependent algorithms for hydrogen enthalpy. The algorithms include the enthalpy gained by converting from para to normal hydrogen between 200 K and 300 K. Turbine inlet temperature, weapon power, weapon-cooling load, and weapon outlet hydrogen temperature are prescribed and are used to calculate the flow rates.

The turbine's flow rate also depends on its pressure ratio, which is optimized to obtain the lowest possible system mass. This pressure ratio also determines the turbine's outlet pressure and temperature. As the pressure ratio increases, less hydrogen is needed by the turbine because more enthalpy is extracted from it, but the turbine gets heavier because stages have to be added to get higher pressure ratios. The optimization procedure trades off mass gains and losses to obtain a minimum system mass.

The model makes the following component efficiency assumptions: turbine efficiency is 90%, generator efficiency is 95%, and power conditioning unit efficiency is 95%. Mass algorithms for the various components are described briefly below.

Hydrogen and oxygen subsystems -- The hydrogen subsystem consists of hydrogen stored at 20 K and 0.1 MPa, a pressure vessel, multilayer insulation, a refrigeration unit, and a meteoroid shield. The mass algorithms for these components are given in Appendix A. The mass of hydrogen needed is equal to the greater of the weapon and turbine flow rates multiplied by the weapon's operation time. Pump power is calculated and is integrated into the flow rate analysis. The oxygen subsystem's mass is calculated in much the same manner as the hydrogen subsystem's mass. The oxygen's flow rate depends on the power required by the weapon, on the turbine's pressure ratio (which is optimized), and on the hydrogen-to-oxygen ratio, which depends on the turbine's inlet temperature.

Reactor and shield -- The algorithms for reactor and shield mass were developed by Marshall (1986). Reactor mass depends on fuel mass with factors added to estimate structure, moderator, pressure vessel, reflector and miscellaneous masses. The algorithm calculates three values for fuel mass: (1) the mass of fuel needed for the reactor to be critical at the end of its life; (2) the fuel needed so that the reactor's burnup fraction limit is not exceeded; and (3) the fuel needed to provide adequate heat transfer surface area for heat removal. The greatest of these three values is used as the reactor's fuel mass. The shield's mass depends on prescribed neutron and gamma dose limits at a prescribed distance from the reactor. (Reactor shields were found to be unnecessary in this study because short operation times led to small radiation doses.)

Turbine mass -- Turbine mass algorithms were developed by Hudson (1988). Each stage of the turbine is sized to get maximum blade and disk speed without exceeding material strength limits. The following assumptions are made:

- Impulse staging has a nozzle-to-blade velocity ratio of 2:1.
- Each stage has a blade-length-to-axial-width radio of 5.0:1.
- The turbine's volume has a density one-half that of a superalloy metal.

Increasing the turbine's pressure ratio increases the number and size of stages and increases the turbine's mass.

Power Conversion Components -- We assumed a generator specific mass of 0.1 kg/kW, which is a typical mass for a generator using current technology. Cryogenically cooled generators may be as light as one-fourth this specific mass. The flywheel stores enough energy to provide full power for 10 s and has an energy density of 100 Wh/kg (0.36 MJ/kg). Power conditioning was assumed to weigh 0.2 kg/kW. This specific mass is too high for an EML weapon, which will require very little power conditioning since it can use the power produced by the turbine directly to run its homopolar generator. However, 0.2 kg/kW may be too low for NPBs and FELs, which will require substantial power conditioning to obtain the 100 kV DC power required to drive RF generators such as klystrodes. The weight assumed for power conditioning does not, however, affect our conclusions since the value we use will be constant and will not depend on turbine inlet temperature.

Miscellaneous components -- Ten percent of the sum of the component weights was added to the system's subtotal mass to account for such things as piping and structure.

RESULTS

Figure 3 shows the resulting system component masses for a 500 MWe reactor-powered system. In this figure, power system specific mass (kg/kW) is presented as a function of turbine inlet temperature. Reactor and turbine masses each represent only 1% of the system's total mass and are not significant for this system. Power conditioning and generator masses are significant. The mass of hydrogen needed by the turbine decreases as turbine inlet temperature increases, but the

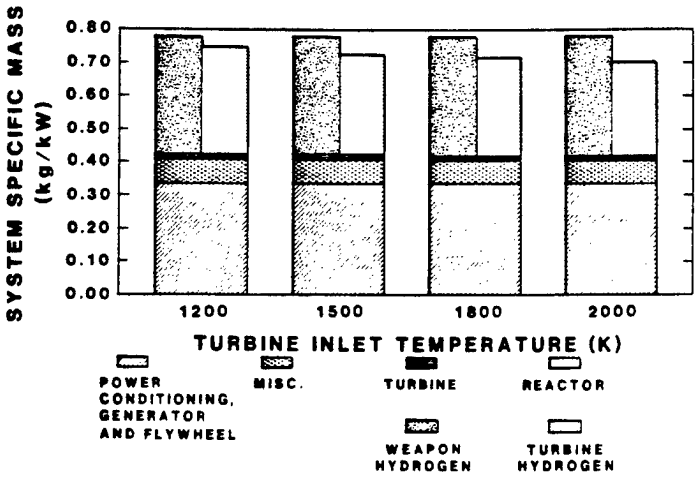

Figure 3. 500 MWe, Burst-Mode, Reactor Power System: 50% Weapon Cooling Load, 300 K Weapon Coolant Outlet Temperature (1800-s operation time, 13.6 MPa turbine inlet pressure)

mass of hydrogen needed by a weapon with a 50% cooling load and a 300 K coolant outlet temperature is greater. Thus, the system mass includes the mass of hydrogen needed by the weapon with no additional amount needed for the turbine. The mass of hydrogen needed by the weapon does not depend on turbine inlet temperature; thus, no significant system mass reduction is derived by using turbine inlet temperatures above 1200 K for this example. Even if the weapon needed less hydrogen than the turbine, less than 0.1 kg/kW would be saved by using a 2000 K instead of a 1200 K turbine inlet temperature.

Similar results for the combustion system are shown in Figure 4. The required mass of oxygen increases with increasing turbine inlet temperature because the proportion of oxygen to hydrogen increases as the combustion temperature increases. The mass of hydrogen required by a weapon with a 50% cooling load and a 300 K coolant outlet temperature is also greater than that required by the turbine for this system.

Because oxygen mass increases as temperature increases, there is actually a mass penalty associated with higher turbine inlet temperatures if the weapon uses more hydrogen than the turbine. Even if the weapon used less hydrogen than the power generation system, the combustion system's mass savings gained by going to higher turbine inlet temperatures is less than 0.1 kg/kW.

As stated earlier, the mass reduction benefits associated with using a higher turbine inlet temperature depend on the weapon's cooling load and coolant outlet temperature for a reactor-powered, burst-mode system. We are considering the weapon's cooling load instead of its efficiency because all weapon inefficiencies do not necessarily generate heat that must be removed by the cooling system. For example, the electron stripper at the end of an NPB weapon

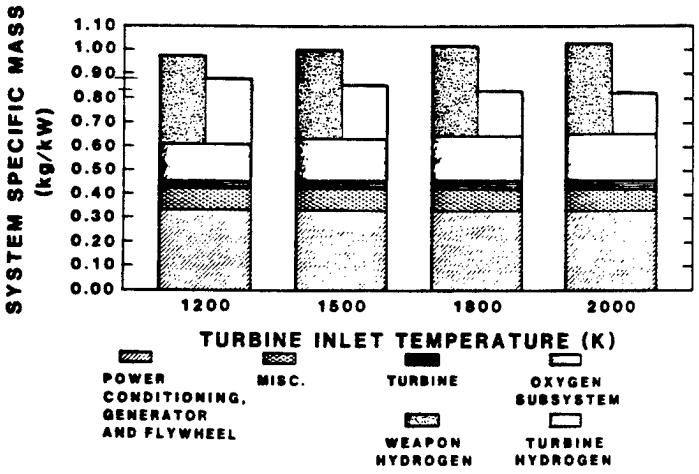

Figure 4. 500 MWe, Burst-Mode, Combustion Power System: 50% Weapon Cooling Load, 300 K Weapon Coolant Outlet Temperature (1800-s operation time, 13.6 MPa turbine inlet pressure)

may cause large inefficiencies (beam scattering and etc.) without introducing a cooling load.

Figure 5 shows the effect turbine inlet temperature has on a reactor-powered system's specific mass for a variety of weapon cooling loads and coolant outlet temperatures. Along the bottom curve the power system needs more hydrogen than the weapon. Curves associated with various weapon cooling loads and outlet temperatures intersect this bottom curve at various points. These intersection points show the "break-even" temperatures where the weapon and the power generation system's turbine need the same quantity of hydrogen. To the left of an intersection point, the power system's turbine needs more hydrogen, and to the right the weapon needs more. The curves are for a 500 MWe system that operates for 1800 s and uses a 13.6 MPa turbine inlet pressure.

To find the system's specific mass for a system with a weapon cooling load of 50% and an outlet temperature of 400 K, we start in the upper left-hand corner of the figure and follow the bottom curve down to where it intersects the curve labeled 50%, 400 K. Then, we follow the 50%, 400 K curve that decreases only slightly as temperature increases. This slight decrease is due to a small reduction in turbine mass at the higher temperatures. Hydrogen mass is constant on this part of the curve because the quantity of hydrogen needed by the weapon does not depend on turbine inlet temperature. As the weapon's cooling load increases or as its outlet temperature decreases, the break-even temperature decreases. It can be seen from the 40%, 300 K and 50%, 400 K curves that turbine inlet temperatures above 1200 to 1300 K do not significantly reduce system mass for these conditions. Unless weapon cooling loads are below 40% to 50% or weapon outlet coolant temperatures are above 300 K to 400 K, there is little to be gained by using turbine inlet temperatures above those achievable with current material technology.

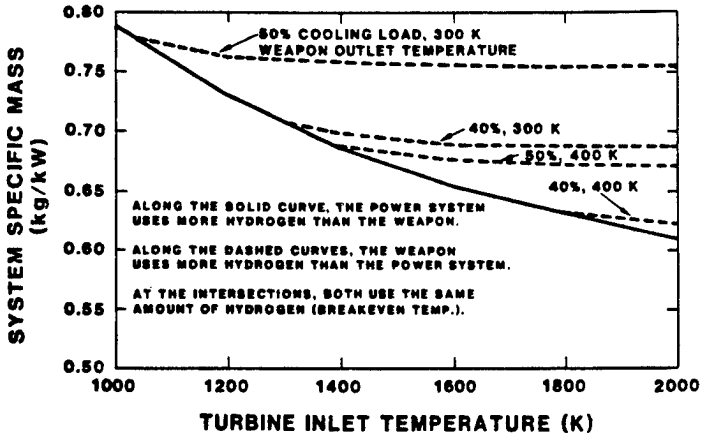

Figure 5. 500 MWe Burst, Reactor Power System: Various Weapon Cooling Loads and Coolant Outlet Temperatures (1800-s operation time, 13.6 MPa turbine inlet pressure)

Current technology uses superalloy turbines that can tolerate temperatures up to about 1350 K without blade cooling or about 1600 K with blade cooling as used in aircraft engines. (The effect of blade cooling on system performance was not considered in this study.)

What are the prospects that weapon cooling loads will be below 40% to 50% or that weapon coolant outlet temperatures will be above 300 K to 400 K? At this time we have not studied weapon cooling in sufficient detail to answer this question. We do know that cooling loads and coolant temperatures are not independent; that is, higher coolant temperatures usually cause greater cooling loads because electrical resistance increases as temperatures increase. The prospects for very low cooling loads, achieved using superconduction, have not been addressed in this study, but superconduction could lead to very low cooling requirements.

So far, results have been shown for a 500 MWe system that operates for 1800 s and uses a turbine inlet pressure of 13.6 MPa. Figure 6 shows the effect of varying power level, operation time, and turbine inlet pressure on the quantity of hydrogen used by a power system's turbine. Hydrogen mass is given in kg/kWh; thus, if hydrogen mass was proportional to only power level and operation time, all of the curves would coincide. The nominal dashed curve in this figure is for the 500 MWe, 1800 s, 13.6 MPa system. The other dashed curves show variations from the nominal. For example, the dashed curve labeled 200 s has changed the operation time but not the other nominal parameters.

The curves do not coincide for two reasons. The first reason can be explained by considering the 1800 s and 200 s systems. The 200 s system uses much less hydrogen. Since its hydrogen mass is relatively low, it can afford to add a little hydrogen in order to make its turbine lighter

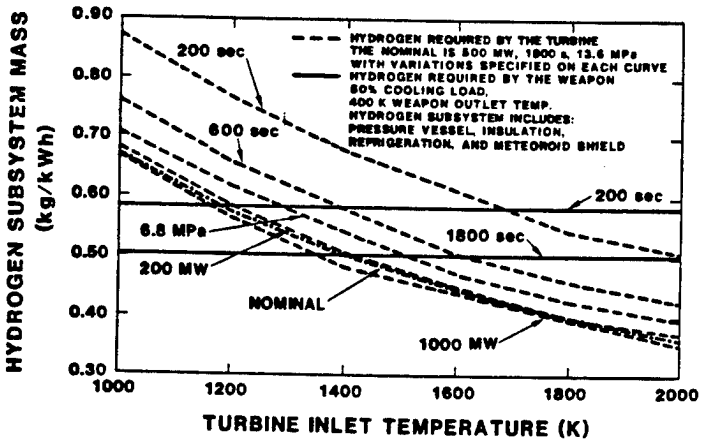

Figure 6. Burst, Reactor Power System Hydrogen Subsystem Mass

by using a lower pressure ratio and avoiding the larger, low-pressure stages. In other words, it trades turbine mass for hydrogen mass. So the first reason the curves do not coincide is because of the system model's optimization procedure. The second reason is that the hydrogen's mass, which includes the pressure vessel, insulation, refrigeration unit, and meteoroid shield, is not directly proportional to its volume and is therefore not proportional to hydrogen mass. This is illustrated in Figure 6 by the two weapon hydrogen requirement lines. One is for an 1800 s and the other is for 200 s operation time. These two lines differ because of the hydrogen subsystem's mass nonlinearity with volume.

From the 200 MWe, nominal, and 1000 MWe curves, we see that hydrogen subsystem mass does not depend strongly on system power level, but it does depend somewhat on turbine inlet pressure, and it depends strongly on operation time. Notice that as operation time decreases, the break-even temperature (the temperature where a solid line and dashed curve intersect) increases. Thus, shorter operation times favor increased turbine inlet temperatures. But unless weapon cooling loads are below those shown in the figure or unless outlet coolant temperatures are somewhat higher, there is little advantage to exceeding current material temperature limits (~1350 K without blade cooling, ~1600 K with blade cooling for superalloys).

CONCLUSIONS

Unless weapon cooling loads can be reduced to below 40% to 50% of weapon power input or unless coolant outlet temperatures above 300 K to 400 K can be used, turbine inlet temperatures exceeding current material technology limits cannot be justified for reactor powered, burst mode space power applications. Higher turbine inlet temperatures cannot be justified for hydrogen-

oxygen combustion-powered systems for any weapon cooling load or coolant outlet temperature.

Two assumptions that need more discussion have been made in arriving at these conclusions:

1. Weapon cooling systems can be designed to operate at 13.6 MPa. Such a high pressure, although a benefit to heat transfer, may require an unacceptable weapon structure mass. If so, the power system must be operated at a lower pressure or hydrogen coolant will have to be compressed after leaving the weapon. In either case, the quantity of hydrogen needed by the power system's turbine will increase and will move the "break-even" temperature (temperature where the power system's turbine and the weapon need the same quantity of hydrogen) to higher values.

2. Oxygen will not be used as a coolant. If oxygen can be used as a coolant, the weapon will require less hydrogen and the "break-even" temperature will be increased.

These conclusions do not carry over into other power conversion applications. (For example, higher turbine inlet temperatures may significantly reduce the weight of a closed, Brayton cycle continuous power system because radiators can be made smaller.) Nor do they imply that because current material technology can be used, that turbine development is unnecessary. The gas turbines needed for burst-mode applications have higher power and need many more stages than current gas turbines, and they will use hydrogen, or hydrogen-oxygen combustion products, instead of air-fuel combustion products as a working fluid.

Appendix A
Hydrogen Subsystem Mass

The hydrogen subsystem mass (labeled hydrogen mass in Figures 3 and 4) includes the masses of hydrogen, a pressure vessel, insulation, a refrigeration system, and a meteoroid shield. The details for this analysis are described in Edenburn (1988). A similar analysis was used for an oxygen storage subsystem.

Hydrogen mass -- The density of liquid hydrogen at 20 K and 0.1 MPa is 71 kg/m^3.

$$\text{Hydrogen mass} = 71 \times V \text{ kg}$$

V is the volume of hydrogen in m^3.

Pressure vessel mass -- A spherical pressure vessel stress analysis prescribes the wall thickness used to determine mass. The following mass algorithm is for a steel pressure vessel at 0.1 MPa with a design stress of 207 MPa.

$$\text{Pressure vessel mass} = 5.7 \times V \text{ kg}$$

The effect of launch forces has not been considered here. Also, we have neglected any structural benefit from the meteoroid shield. It is possible that the structural characteristics of the shield can be integrated with the pressure vessel so that launch forces are accommodated.

Insulation mass -- Multifoil insulation has a density of 80 kg/m^3 and a conductivity between 0.00004 and 0.0002 W/mK. We used 0.0001 W/mK. The hydrogen's temperature is 20 K and space temperature is 250 K. Using these figures the heat gain is equal to 0.96 W/m^2. An insulation thickness of 2.4 cm minimizes the sum of refrigeration system and insulation masses.

$$\text{Insulation mass} = 9.3 \times V^{.667} \text{ kg}$$

Refrigeration system mass -- This system consists of a power system, refrigeration equipment, and a refrigeration radiator. The coefficient of performance (COP) for the refrigeration system is assumed to be 0.2 times that of a Carnot refrigerator. The power system for the refrigerator was assumed to be a Rankine cycle system, and its mass was found using Sandia's reference system model RNKCYC (Edenburn 1988). The refrigeration cycle radiator was assumed to have a mass of 5 kg/m^2 and to operate at 400 K, which minimizes the sum of power system, refrigeration equipment, and radiator masses. The refrigeration equipment was assumed to have a mass of 4 kg/kW. Refrigeration equipment consists of compressors, heat exchangers, and vapor separators in a multiloop cascaded cycle.

$$\text{Refrigeration system mass} = 9.1 \times V^{.667} \text{ kg}$$

Meteoroid shield -- The meteoroid shield is aluminum and is designed for low Earth orbit (1000 km) and a seven-year life. The algorithm used to determine shield thickness is taken from Fraas (1986). The shield assumed in this calculation will not protect against space debris since such a shield would be prohibitively massive.

$$\text{Shield mass} = 107 \times V^{.86} \text{ kg}$$

For more detail see Edenburn (1988).

References

Edenburn, M. W. (1988), Models for Multimegawatt Space Power Systems, SAND86-2742, Sandia National Laboratories, Albuquerque, NM., to be published.

Fraas, A. C. (1986), Protection of Spacecraft from Meteoroids and Orbital Debris, ORNL/TM 9904, Oak Ridge National Laboratory, Oak Ridge, TN, February 1986.

Hudson, S. L. (1988), "Hydrogen Turbines for Space Power Systems: A Simplified Axial Flow Gas Turbine Model," 5th Symposium on Space Nuclear Power Systems, January 1988, Albuquerque, New Mexico.

Marshall, A. C. (1986), RSMASS: A Preliminary Reactor/Shield Mass Model for SDI Applications, SAND86-1020, Sandia National Laboratories, Albuquerque, NM, August 1986.

DISTRIBUTION

AFAT/SAS
Fort Walton Beach, FL 32542
Attn: Capt. Jerry Brown

AFISC/SNAR
Kirtland Air Force Base
New Mexico 87117
Attn: Lt. Col. J. P. Joyce

AF Astronautics Laboratory/LKCJ
Edwards Air Force Base
MS 24
California 93523
Attn: G. Beale

AF Astronautics Laboratory/LKCJ
Edwards Air Force Base
California 93523
Attn: F. Meade

AF Astronautics Laboratory/LKCJ
Edwards Air Force Base
California 93523
Attn: Lt. R. Henley

AF Astronautics Laboratory/LKCJ
Edwards Air Force Base
California 93523
Attn: Major E. Houston

AFWAL/AA
Wright-Patterson AFB
Ohio 45433
Attn: Dick Renski

AFWAL/POOS
Wright-Patterson AFB
Bldg. 450
Ohio 45433
Attn: E. B. Kennel

AFWAL/POOC-1
Bldg. 450
Wright-Patterson AF Base
Ohio 45433
Attn: R. Thibodeau

AFWAL/POO
Aeronautical Laboratory
Wright-Patterson AFB
Ohio 45433
Attn: W. Borger

Aeronautical Laboratory
Bldg. 18
Wright-Patterson AFB
Ohio 45433
Attn: P. Colgrove

AFWAL/POOC-1
Aero-Propulsion Laboratory
Bldg. 450
Wright-Patterson AFB
Ohio 45433
Attn: D. Massie

AFWAL/POOC-1
Aeronautical Laboratory
Wright-Patterson AFB
Ohio 45433
Attn: C. Oberly

AFWAL/POOC-1
Aeronautical Laboratory
Wright-Patterson AFB
Ohio 45433
Attn: T. Mahefky

AFWAL/POOS
Wright-Patterson AFB
Ohio 45433
Attn: J. Beam

AFWAL/POOC-1
Power Components Branch
Wright Patterson AFB
Ohio 45433-6563

AFWAL/POOC
Aeronautical Laboratory
Bldg. 18
Wright-Patterson AFB
Ohio 45433
Attn: Major Seward

AFWL/AFSC
Kirtland Air Force Base
New Mexico 87117
Attn: M. J. Schuller

AFWL/AW
Kirtland AFB
New Mexico 87117
Attn: Dr. D. Kelleher

AFWL
Kirtland Air Force Base
New Mexico 87117
Attn: Lt. Col. Jackson

AFWL
Kirtland Air Force Base
New Mexico 87117
Attn: Dr. Frank Jankowski

AFWL
Kirtland Air Force Base
New Mexico 87117
Attn: Dr. Charles Terrell

AFWL
Kirtland Air Force Base
New Mexico 87117
Attn: Dr. M. J. Schuller

AFSTC
Kirtland Air Force Base
New Mexico 87117
Attn: Lt. Col. Phillip Newton

AFSTC
Kirtland Air Force Base
New Mexico 87117
Attn: Mr. Gregory Powers

AFWL/AWYS
Kirtland Air Force Base
New Mexico 87117
Attn: Major D. R. Boyle

HQ AFSPACECOM/XPXIS
Peterson Air Force Base
Colorado 80914-5001
Attn: Lt. Col. F. Lawrence

HQ USAF/RD-D
Washington, DC 20330-5042
Attn: Maj. P. Talty

Aerospace Corporation
Bldg. 497, Rm. 123
P. O. Box 9113
Albuquerque, NM 87119
Attn: W. Zelinski

Aerospace Corporation
P. O. Box 9113
Albuquerque, NM 87119
Attn: W. Blocker

Aerospace Corporation
P. O. Box 9113
Albuquerque, NM 87119
Attn: M. Firmin

Aerospace Corporation
P. O. Box 92957
El Segundo, CA 90009
Attn: P. Margolis

Air Force Center for Studies
and Analyses/SASD
The Pentagon, Room ID-431
Washington, DC 20330-5420
Attn: W. Barattino, AFCSA/SASD

Air Force Foreign Technology Div.
TQTD
Wright-Patterson AFB
Ohio 45433-6563
Attn: Dr. B. L. Ballard

AFWL/AWYS
Kirtland AFB
New Mexico 87117
Attn: Major D.R. Ballard

TQTD
Wright-Patterson AFB
Ohio 45433-6563
Attn: K. W. Hoffman

Air Force Space Technology Center
SWL
Kirtland AFB, NM 87117-6008
Attn: Capt. M. Brasher

Air Force Space Technology Center
SWL
Kirtland AFB, NM 87117-6008
Attn: J. DiTucci

Air Force Space Technology Center
SWL
Kirtland AFB, NM 87117-6008
Attn: Capt. E. Fornoles

Air Force Space Technology Center
TP
Kirtland AFB, NM 87117-6008
Attn: M. Good

Air Force Space Technology Center
XLP
Kirtland AFB, NM 87117-6008
Attn: A. Huber

Air Force Space Technology Center
SWL
Kirtland AFB, NM 87117-6008
Attn: Capt. S. Peterson

ANSER Corp.
Crystal Gateway 3
1225 Jefferson Davis Highway #800
Arlington, VA 22208
Attn: K. C. Hartkay

Argonne National Laboratory
9700 S. Cass Avenue
Argonne, IL 60439
Attn: Dr. Samit K. Bhattacharyya

Argonne National Laboratory
9700 S. Cass Avenue
Argonne, IL 60439
Attn: D. C. Fee

Argonne National Laboratory
9700 S. Cass Avenue
Argonne, IL 60439
Attn: K. D. Kuczen

Argonne National Laboratory
9700 S. Cass Avenue
Argonne, IL 60439
Attn: Dr. R. A. Lewis

Argonne National Laboratory
9700 S. Cass Avenue
Argonne, IL 60439
Attn: D. C. Wade

Auburn University
202 Sanform Hall
Auburn, AL 36849-3501
Attn: Dr. T. Hyder

Auburn University
231 Leach Center
Auburn, AL 36849-3501
Attn: Dr. F. Rose

Avco Research Laboratory
2385 Revere Beach Pkwy
Everett, Mass. 02149
Attn: D. W. Swallom

Babcock & Wilcox
Nuclear Power Division
3315 Old Forest Road
P.O. Box 10935
Lynchburg, VA 24506-0935
Attn: B. J. Short

Battelle Pacific Northwest Lab.
P. O. Box 999
Richland, WA 99352
Attn: J. O. Barner

Battelle Pacific Northwest Lab.
P. O. Box 999
Richland, WA 99352
Attn: Dr. L. Schmid

Battelle Pacific Northwest Lab.
P. O. Box 999
Richland, WA 99352
Attn: E. P. Coomes

Battelle Pacific Northwest Lab.
P.O. Box 999
Richland, WA 99352
Attn: B. M. Johnson

Battelle Pacific Northwest Lab.
P. O. Box 999
Richland, WA 99352
Attn: W. J. Krotiuk

Battelle Pacific Northwest Lab.
P. O. Box 999
Richland, WA 99352
Attn: W. J. Widrig

The BDM Corporation
7915 Jones Branch Dr.
M.S. West Branch 5B37
McLean, VA 22102-3396
Attn: Dr. Ehsan Khan

The BDM Corporation
1801 Randolph Road SE
M.S. BV-24
Albuquerque, NM 87106
Attn: D. E. Jackson

Boeing Company
P.O. Box 3999
MS 8K-30
Seattle, WA 98124-2499
Attn: Dr. A. Sutey

Boeing Company
Boeing Aerospace System
P.O. Box 3707
Seattle, WA 98124
Attn: K. Kennerud

Brookhaven National Laboratory
P.O. Box 155
Upton, NY 11973
Attn: T. Bowden

Brookhaven National Laboratory
P.O. Box 155
Upton, NY 11973
Attn: H. Ludewig

Brookhaven National Laboratory
P.O. Box 155
Upton, NY 11973
Attn: Dr. W. Y. Kato

Brookhaven National Laboratory
Bldg. 701, Level 143
MS 820M
P.O. Box 155
Upton, NY 11973
Attn: Dr. J. Powell

California Inst. of Technology
Jet Propulsion Laboratory
4800 Oak Grove Drive
Pasadena, CA 91109
Attn: V. C. Truscello

Jet Propulsion Laboratory
4800 Oak Grove Drive
MS 122-123
Pasadena, CA 91109
Attn: P. Bankston

California Inst. of Technology
Jet Propulsion Laboratory
MS 502-307
4800 Oak Grove Drive
Pasadena, CA 91109
Attn: E. P. Framan

California Inst. of Technology
Jet Propulsion Laboratory
MS 264-770
4800 Oak Grove Drive
Pasadena, CA 91109
Attn: L. Isenberg

California Inst. of Technology
Jet Propulsion Laboratory
4800 Oak Grove Drive
Pasadena, CA 91109
Attn: J. Mondt

DARPA
1400 Wilson Blvd.
Arlington, VA 22209
Attn: P. Kemmey

DCSCON Consulting
4265 Drake Court
Livermore, CA 94550
Attn: D. C. Sewell

Defense Nuclear Agency
6801 Telegraph Road
Alexandria, VA 22310-3398
Attn: J. Farber/RAEV

DNA/RAEV
6801 Telegraph Road
Alexandria, VA 22310-3398
Attn: J. Foster

EG&G Idaho, Inc./INEL
P.O. Box 1625
Idaho Falls, ID 83415
Attn: John S. Martinell

EG&G Idaho, Inc./INEL
P.O. Box 1625
Idaho Falls, ID 83415
Attn: J. Dearien

EG&G Idaho, Inc./INEL
P.O. Box 1625
Idaho Falls, ID 83415
Attn: M. L. Stanley

EG&G Idaho, Inc./INEL
P.O. Box 1625
Idaho Falls, ID 83415
Attn: R. D. Struthers

EG&G Idaho, Inc./INEL
P.O. Box 1625
Idaho Falls, ID 83415
Attn: J. F. Whitbeck

EG&G Idaho, Inc./INEL
P.O. Box 1625
Idaho Falls, ID 83415
Attn: P. W. Dickson

EG&G Idaho, Inc./INEL
P.O. Box 1625
Idaho Falls, ID 83415
Attn: J. W. Henscheid

Ford Aerospace Corporation
Aeronutronic Div.
Ford Road, P.O. Box A
Newport Beach, CA 92658-9983
Attn: V. Pizzuro

GA Technologies
P.O. Box 85608
San Diego, CA 92138
Attn: H. J. Snyder

GA Technologies
P.O. Box 85608
San Diego, CA 92138
Attn: C. Fisher

GA Technologies
P.O. Box 85608
San Diego, CA 92138
Attn: Dr. R. Dahlberg

Garrett Fluid Systems Co.
P.O. Box 5217
Phoenix, AZ
Attn: Robert Boyle

General Electric
P. O. Box 8555
Astro Systems
Philadelphia, PA 19101
Attn: Dr. R. J. Katucki

General Electric NSTO
310 DeGuigne Drive
Sunnyvale, CA 90486
Attn: E. E. Gerrels

General Electric NSTO
310 DeGuigne Drive
Sunnyvale, CA 90486
Attn: H. S. Bailey

General Electric-SCO
P. O. Box 8555
35T15, Bldg. 20
Astro Systems
Philadelphia, PA 19101
Attn: J. Chan

General Electric
P. O. Box 8555
Bldg. 100, Rm M2412
Astro Systems
Philadelphia, PA 19101
Attn: J. Hnat

General Electric
P. O. Box 8555
Astro Systems
Philadelphia, PA 19101
Attn: R. D. Casagrande

General Electric
P. O. Box 8555
Astro Systems
Philadelphia, PA 19101
Attn: W. Chiu

Grumman Aerospace Corporation
MS B20-05
Bethpage, NY 11714
Attn: J. Belisle

Horizon Systems
575 Bell Ave.
Livermore, CA 94550
Attn: Dr. William Wright

House of Representatives Staff
Space and Technology Committee
2320 Rayburn Building
Washington, DC 20515
Attn: Tom Weimer

INSPI
202 NSC
University of Florida
Gainesville, FL 32611
Attn: N. J. Diaz

ERC International
1717 Louisiana NE
Suite 202
Albuquerque, NM 87110
Attn: W. H. Roach

ERC International
1717 Louisiana NE
Suite 202
Albuquerque, NM 87110
Attn: G. B. Varnado

ERC International
1717 Louisiana NE
Suite 202
Albuquerque, NM 87110
Attn: D. M. Ericson

Lawrence Livermore National Lab.
P. O. Box 808
Livermore, CA 94550
Attn: Lynn Cleland, MS L-144

Lawrence Livermore National Lab.
P. O. Box 808
Livermore, CA 94550
Attn: C. E. Walter, MS L-144

Los Alamos National Laboratory
P. O. Box 1663
Los Alamos, NM 87545
Attn: T. Trapp, MS-E561

Los Alamos National Laboratory
P. O. Box 1663
Los Alamos, NM 87545
Attn: R. Hardie, MS-F611

Los Alamos National Laboratory
P. O. Box 1663
Los Alamos, NM 87545
Attn: C. Bell, MS F611

Los Alamos National Laboratory
P. O. Box 1663
Los Alamos, NM 87545
Attn: R. J. LeClaire, MS F611

Los Alamos National Laboratory
P. O. Box 1663
Los Alamos, NM 87545
Attn: S. Jackson, MS-F611

Los Alamos National Laboratory
P. O. Box 1663
Los Alamos, NM 87545
Attn: J. Metzger

Los Alamos National Laboratory
P. O. Box 1663
Los Alamos, NM 87545
Attn: C. W. Watson, MS-F607

Los Alamos National Laboratory
P. O. Box 1663
Los Alamos, NM 87545
Attn: Don Reid, MS-H811

Los Alamos National Laboratory
P. O. Box 1663
Los Alamos, NM 87545
Attn: R. Bohl, MS-K560

Los Alamos National Laboratory
P. O. Box 1663
Los Alamos, NM 87545
Attn: D. R. Bennett

Los Alamos National Laboratory
P. O. Box 1663
Los Alamos, NM 87545
Attn: W. L. Kirk

Los Alamos National Laboratory
P. O. Box 1663
Los Alamos, NM 87545
Attn: M. Merrigan

Los Alamos National Laboratory
P. O. Box 1663
Los Alamos, NM 87545
Attn: T. P. Suchocki

Los Alamos National Laboratory
P. O. Box 1663
Los Alamos, NM 87545
Attn: L. H. Sullivan

Martin Marietta Corp.
P. O. Box 179
Denver, CO 80201
Attn: R. Giellis, MS 0484

Martin Marietta Corp.
P. O. Box 179
Denver, CO 80201
Attn: R. Zercher
MSL8060

Massachusetts Institute of
Technology
1328 Albany Street
Cambridge, MA 02139
Attn: Dr. J. A. Bernard

NASA Lewis Research Center
21000 Brookpark Road
Cleveland, OH 44135
Attn: J. Winter, MS 301-5

NASA Lewis Research Center
21000 Brookpark Road
Cleveland, OH 44135
Attn: Barbara McKissock, MS 301-5

NASA Lewis Research Center
21000 Brookpark Road
Cleveland, OH 44135
Attn: A. Juhasz
MS 301-5, Rm. 101

NASA Lewis Research Center
21000 Brookpark Road
Cleveland, OH 44135
Attn: J. Smith, MS 301-5

NASA Lewis Research Center
21000 Brookpark Road
Cleveland, OH 44135
Attn: H. Bloomfield
MS 301-5, Rm. 103

NASA Lewis Research Center
21000 Brookpark Road
Cleveland, OH 44135
Attn: Jim Bolander, 3350
Research/Technology Branch

NASA Lewis Research Center
21000 Brookpark Road
Cleveland, OH 44135
Attn: Kathleen Batke; 3350
Research/Technology Branch

NASA Lewis Research Center
21000 Brookpark Road
Cleveland, OH 44135
Attn: C. Purvis
MS 302-1, Rm. 101

NASA Lewis Research Center
21000 Brookpark Road
Cleveland, OH 44135
Attn: Dr. Dennis Flood
MS 302-1

NASA Lewis Research Center
21000 Brookpark Road
Cleveland, OH 44135
Attn: D. Bents, MS 301-5

NASA Lewis Research Center
21000 Brookpark Road
Cleveland, OH 44135
Attn: I. Myers
MS 301-2, Rm 116

NASA Lewis Research Center
21000 Brookpark Road
Cleveland, OH 44135
Attn: G. Schwarze MS 301-2, Rm. 117

NASA Lewis Research Center
21000 Brookpark Road
Cleveland, OH 44135
Attn: J. Sovie MS 301-5, Rm. 105

National Research Council
Energy Engineering Board
Commission on Engineering
and Technical Systems
2101 Constitution Avenue
Washington, DC 20418
Attn: R. Cohen

Naval Research Laboratory
Washington, DC 20375-5000
Attn: R. L. Eilbert

Naval Research Laboratory
Washington, DC 20375-5000
Attn: I. M. Vitkovitsky

Naval Space Command
Dahlgren, VA 22448
Attn: Commander R. Nosco

Naval Space Command
N5
Dahlgren, VA 22448
Attn: Maj. J. Wiley

Naval Space Command
Dahlgren, VA 22448
Attn: Mr. B. Meyers

Naval Surface Weapons Center
Code F-12
Dahlgren, VA 22448-5000
Attn: Mr. Lawrence Luessen

Naval Surface Weapons Center
Dahlgren, VA 22448-5000
Attn: R. Gripshoven-F12

Naval Surface Weapons Center
Dahlgren, VA 22448-5000
Attn: R. Dewitt-F12

White Oak Laboratory
Silver Springs, MD 20903-500
MC R-42
Attn: B. Maccabee

Nichols Research Corp.
2340 Alamo Street, SE
Suite 105
Albuquerque, NM 87106
Attn: R. Weed

Oak Ridge National Laboratory
P. O. Box Y
Bldg. 9201-3, MS-7
Oak Ridge, TN 37831
Attn: J. P. Nichols

Oak Ridge National Laboratory
P. O. Box Y
Bldg. 9201-3, MS-7
Oak Ridge, TN 37831
Attn: D. Bartine

Oak Ridge National Laboratory
P. O. Box X
Oak Ridge, TN 37831
Attn: H. W. Hoffman

Oak Ridge National Laboratory
P. O. Box Y
Bldg. 9201-3, MS-7
Oak Ridge, TN 37831
Attn: R. H. Cooper, Jr.

Oak Ridge National Laboratory
P. O. Box Y
Bldg. 9201-3, MS-7
Oak Ridge, TN 37831
Attn: J. C. Moyers

Oak Ridge National Laboratory
P. O. Box Y
Oak Ridge, TN 37831
Attn: M. Olszewski

Oak Ridge National Laboratory
P. O. Box Y
Bldg. 9201-3, MS-7
Oak Ridge, TN 37831
Attn: M. Siman-Tov

Oak Ridge National Laboratory
P. O. Box Y
Bldg. 9201-3, MS-7
Oak Ridge, TN 37831
Attn: F. W. Wiffen

RADC/OCTP
Griffiss AFB
New York 13441
Attn: R. Gray

Riverside Research Institute
1701 No. Ft. Meyers Drive
Suite 700
Arlington, VA 22209
Attn: J. Feig

Science & Engineering Associates
6301 Indian School Road, NE
Albuquerque, NM 87110
Attn: G. L. Zigler

SDI Organization
The Pentagon
Washington, DC 20301-7100
Attn: R. Verga

SDI Organization
The Pentagon
Washington, DC 20301-7100
Attn: D. Buden

SDI/SLKT
The Pentagon
1717 H. St. NW
Washington, D. C. 20301
Attn: C. Northrup

SDIO/DE
Washington, DC 20301-7100
Attn: Dr. R. Hammond

SDIO/IST
Washington, DC 20301-7100
Attn: Dr. L. Cavery

SDIO/KE
The Pentagon
Washington, DC 20301-7100
Attn: Col. R. Ross

SDIO
The Pentagon
Washington, DC 20301-7100
Attn: Maj. R. X. Lenard

SDIO/SATKA
Washington, DC 20301-7100
Attn: Col. Garry Schnelzer

SDIO/SY
Washington, DC 20301-7100
Attn: Dr. C. Sharn

SDIO/SY
Washington, DC 20301-7100
Attn: Col. J. Schofield

SDIO/SY
Washington, DC 20301-7100
Attn: Col. J. Graham

SDIO/SY
Washington, DC 20301-7100
Attn: Capt. J. Doegan

Space Power, Inc.
1977 Councourse Dr.
San Jose, CA 95131
Attn: J. R. Wetch

State University of New York
at Buffalo
Dept. of Elec. Engineering
312 Bonner Avenue
Buffalo, NY 14260
Attn: Jim Sargeant

TRW
One Space Park
Redondo Beach, CA 90278
Attn: R. L. Hammel

TRW
One Space Park
Redondo Beach, CA 90278
Attn: T. Fitzgerald

TRW
One Space Park
Redondo Beach, CA 90278
Attn: James Garner

One Space Park
Redondo Beach, CA 90278
Attn: B. Glasgow

TRW
One Space Park
Redondo Beach, CA 90278
Attn: A. D. Schoenfeld

Teledyne Brown Engineering
Cummings Research Park
Huntsville, AL 35807
Attn: Dan DeLong

Texas A&M University
Nuclear Engineering Dept.
College Station, TX 77843-3133
Attn: F. Best

Texas Tech. University
Dept. of Electrical Engr.
Lubbock, TX 79409
Attn: Dr. W. Portnoy

U. S. Army ARDC
Building 329
Picatinny Arsenal
New Jersey 87806-5000
Attn: SMCAR-SSA-E

U. S. Army Belvoir RDE Center
Fort Belvoir, VA 22060-5606
Attn: Dr. L. Amstutz-STRABE-FGE

U. S. Army Lab. Com.
SLKET/ML
Pulse Power Technology Branch
Fort Monmouth, NJ 07703-5000
Attn: S. Levy

U. S. Army Lab. Com.
SLKET/ML
Pulse Power Technology Branch
Fort Monmouth, NJ 07703-5000
Attn: N. Wilson

U. S. Army Strategic Defense Com.
106 Wynn Drive
Huntsville, AL 35807
Attn: C. Cooper

U. S. Army Strategic Defense Com.
106 Wynn Drive
Huntsville, AL 35807
Attn: G. Edlin

U. S. Army Strategic Defense Com.
106 Wynn Drive
Huntsville, AL 35807
Attn: R. Hall

U. S. Army Strategic Defense Com.
106 Wynn Drive
Huntsville, AL 35807
Attn: E. L. Wilkinson

U. S. Army Strategic Defense Com.
106 Wynn Drive
Huntsville, AL 35807
Attn: D. Bouska

U. S. Army Strategic Defense Com.
106 Wynn Drive
Huntsville, AL 35807
Attn: W. Sullivan

U. S. Army Strategic Defense Com.
106 Wynn Drive
Huntsville, AL 35807
Attn: F. King

U. S. Department of Energy
Chicago Operations Office
9800 S. Cass Avenue
Argonne, IL 60439
Attn: J. L. Hooper

U. S. Department of Energy
NE-52
GTN
Germantown, MD 20545
Attn: J. Warren

U. S. Department of Energy
NE-54
F415/GTN
Germantown, MD 20545
Attn: E. Wahlquist

San Francisco Operations Office
1333 Broadway Ave,
Oakland, CA 94612
Attn: J. K. Hartman

U. S. Department of Energy
SAN - ACR Division
1333 Broadway
Oakland, CA 94612
Attn: J. Krupa

U. S. Department of Energy
SAN - ACR Division
1333 Broadway
Oakland, CA 94612
Attn: W. Lambert

U. S. Department of Energy
SAN - ACR Division
1333 Broadway
Oakland, CA 94612
Attn: J. Zielinski

U. S. Department of Energy
Pittsburgh Energy Tech. Center
P.O. Box 18288
Pittsburgh, PA 15236
Attn: G. Staats (PM-20)

U. S. Department of Energy
NE-54
Washington, DC 20545
Attn: I. Helms

U. S. Department of Energy
Oak Ridge Operations Office
P.O. Box E
Oak Ridge, TN 37830
Attn: E. E. Hoffman

U. S. Department of Energy
Washington, DC 20545
Attn: S. J. Lanes

U. S. Department of Energy
MA 206
Washington, DC 20545
Attn: J. P. Lee

U. S. Department of Energy
San Francisco Operations Office
1333 Broadway Avenue
Oakland, CA 94612
Attn: S. L. Samuelson

U. S. Department of Energy
ALO/ETD
P.O. Box 5400
Albuquerque, NM 87115
Attn: R. L. Holton

U. S. Department of Energy
ALO/ETD
P.O. Box 5400
Albuquerque, NM 87115
Attn: C. Quinn

U. S. Department of Energy/Idaho
785 DOE Place
Idaho Falls, ID 83402
Attn: P. J. Dirkmaat

United Technologies
International Fuel Cells
195 Governor's Highway
South Windsor, CT 06074
Attn: D. McVay

United Technologies
International Fuel Cells
195 Governor's Highway
South Windsor, CT 06074
Attn: J. L. Preston, Jr.

United Technologies
International Fuel Cells
195 Governor's Highway
South Windsor, CT 06074
Attn: J. C. Trocciola

University of Missouri - Rolla
220 Engineering Research Lab
Rolla, MO 65401-0249
Attn: A. S. Kumar

University of New Mexico
Chemical and Nuclear Engineering
Department
Albuquerque, NM 87131
Attn: M. El-Genk

University of Wisconsin
Fussion Technology Institute
1500 Johnson Drive
Madison, WI 53706-1687
Attn: Gerald Kulcinski

W. J. Schafer Associates
1901 No. Ft. Myers Drive
Suite 800
Arlington, VA 22209
Attn: P. Mace

W. J. Schafer Associates
1901 No. Ft. Myers Drive
Suite 800
Arlington, VA 22209
Attn: Ormon Bassett

W. J. Schafer Associates
1901 No. Ft. Myers Drive
Suite 800
Arlington, VA 22209
Attn: M. Nikolich

W. J. Schafer Associates
1901 No. Ft. Myers Drive
Suite 800
Arlington, VA 22209
Attn: J. Crissey

W. J. Schafer Associates
2000 Randolph Road, SE
#205
Albuquerque, NM 87106
Attn: D. C. Straw

W. J. Schafer Associates
1901 No. Ft. Myers Drive
Suite 800
Arlington, VA 22209
Attn: A. K. Hyder

W. J. Schafer Associates
1901 No. Ft. Myers Drive
Suite 800
Arlington, VA 22209
Attn: Jerry Bueck

Westinghouse Electric
P. O. Box 158
Madison, PA 15663-0158
Attn: J. Chi

Westinghouse
Advanced Energy Systems Division
Manager, Space & Defense Program
Route 70, Madison Exit
Madison, PA 15663
Attn: J. F. Wett

Westinghouse
Advanced Energy Systems Division
P.O. Box 158
Madison, PA 15663
Attn: Dr. J. W. H. Chi

1310 Beulah Road
Bldg. 501-3Y56
Pittsburgh, PA 15235
Attn: J. R. Repp

Westinghouse R&D
1310 Beulah Road
Bldg. 501-3Y56
Pittsburgh, PA 15235
Attn: L. Long

Westinghouse R&D
1310 Beulah Road
Bldg. 501-3Y56
Pittsburgh, PA 15235
Attn: Owen Taylor

Westinghouse Advanced Energy
Systems Division
P.O. Box 158
Madison, PA 15663
Attn: G. Farbman

Westinghouse Hanford Company
P. O. Box 1970
Richland, WA 99352
Attn: D. S. Dutt

Westinghouse Hanford Company
P. O. Box 1970
Richland, WA 99352
Attn: B. J. Makenas

Mr. Robert Wiley
5998 Camelback Lane
Columbia, MD 21045

1200 J. P. Van Devender
1240 K. Prestwich
1248 M. Buttram
1270 R. Miller
1271 M. Clauser
1512 D. Rader
1800 R. Schwoebel
1810 G. Kepler
1830 M. Davis
1832 W. Jones
1832 R. Salzbrenner
1840 R. Eagan
2110 R. Bair
2120 W. Dawes, Jr.
2140 C. Gibbon
2150 E. Graham, Jr.
2560 J. Cutchen
3141 S. A. Landenberger (5)
3151 W. L. Garner (3)
3154-1 C. H. Dalin (8) for DOE/OSTI
6400 D. McCloskey
6410 N. Ortiz
6416 J. Philbin
6420 J. Walker
6421 P. Pickard
6422 J. Brockmann
6425 W. Camp
6440 D. Dahlgren
6450 T. Schmidt
6500 A. W. Snyder
6510 W. Gauster
6511 L. Cropp
6511 M. Edenburn
6511 D. Gallup
6511 S. Hudson
6511 A. Marshall
6511 W. McCulloch
6511 P. McDaniel
6511 R. Pepping
6511 F. Thome
6512 E. Haskin
6512 F. Wyant
6512 M. Chu
6512 D. Dobranich
6512 V. Dandini
8400 R. Wayne
8524 P. W. Dean
9000 R. Hagengruber
9010 W. C. Hines
9012 J. Keizur
9012 L. Connell
9012 R. Zazworski
9100 R. Clem
9110 P. Stokes
9140 D. Rigali